ELSEVIER

Journal of Alloys and Compounds 446–447 (2007) 255–259

Journal of ALLOYS AND COMPOUNDS

www.elsevier.com/locate/jallcom

Ti EELS standards for identification of catalytic species in $NaAlH_4$ hydrogen storage materials

D.D. Graham [a], L.F. Culnane [b], M. Sulic [b], C.M. Jensen [b], I.M. Robertson [a,*]

[a] *University of Illinois, Urbana-Champaign, 1304 W. Green St., Urbana, IL 61801, United States*
[b] *University of Hawai'i, 2545 The Mall, Honolulu, HI 96822-2275, United States*

Received 31 October 2006; received in revised form 2 April 2007; accepted 10 April 2007
Available online 24 April 2007

Abstract

Titanium-catalyzed sodium–aluminum hydride has been studied by using in situ TEM heating experiments in conjunction with electron energy loss spectroscopy and X-ray energy dispersive spectroscopy. Electron energy loss spectroscopy (EELS) standards of Ti, TiO_2, Ti_3Al, cubic Al_3Ti, orthorhombic Al_3Ti, TiH_2, and $TiCl_3$ were prepared and analyzed to enable identification of the form of Ti and how it changes as a function of the number of hydrogenation–dehydrogenation cycles. The $TiCl_3$ precursor in $NaAlH_4$ when cycled at 3 wt.% H_2 capacity remains after 5 cycles but is eliminated by the 10th cycle. The dominant form of Ti is then cubic Al_3Ti. The number of cycles required to achieve this depends on the cycled capacity, with partially cycled requiring more cycles than fully cycled material. The form and location of the Ti responsible for the enhanced performance was not discovered which has implications for the effective amount of Ti. The effects of the electron beam and exposure to air on the particles are shown and discussed.

Keywords: Metal hydrides; Transmission electron microscopy

1. Introduction

The reversibility of $NaAlH_4$ through addition of Ti renewed interest in Na-alanate systems [1–20] despite the fact that these materials do not have sufficient reversible hydrogen storage capacity to meet the Department of Energy system storage requirements for automotive applications. Although significant effort has been made to identify and understand the role of Ti, an outstanding, and arguably the most important, question is the location and form of the Ti that is responsible for the improved hydrogen adsorption/desorption kinetics. Discovering the enhancement process(es) in Ti-doped $NaAlH_4$ remains important to the development of complex light-weight metal hydrides systems as all are thermodynamically and kinetically limited.

From the previous work on Ti-doped $NaAlH_4$, it is known that since Na and Ti are immiscible, an alloy with them as the primary constituents is not expected [21] and that various Al–Ti alloy compositions (Al_3Ti, $Al_{1-x}Ti_x$, $x = 0.07$) [22–24] form irrespective of the form of the precursor used to introduce Ti. The dominant form of Ti after multiple hydrogen charging and discharging cycles is Al_3Ti, although a distorted hexagonal close-packed Ti has been identified too [22,25]. Electron paramagnetic resonance spectra indicate that, in bulk samples, Ti^{3+} is reduced to Ti^0 after a few cycles [14]. Scanning electron microscopy in combination with X-ray energy dispersive spectroscopy (EDS) performed on dehydrided $NaAlH_4$ (doped with 2 mol% $Ti(OBu^n)_4$) after five cycles suggests a correlation between Al and Ti with separated Na nodules [26]. Prior work with transmission electron microscopy (TEM) analysis of $LiAlH_4 + 2$ mol% TiF_3 concluded that Ti was in the form of TiO_2 [27], while TEM analysis of $NaAlH_4 + 2$ mol% TiF_3 indicated that, following several dehydrogenation/rehydrogenation cycles, the Ti was correlated with Al [28].

This paper reports on the chemical analysis of $NaAlH_4 + 2$ mol% $TiCl_3$ using electron energy loss spectrometry (EELS) and energy dispersive X-ray spectroscopy to determine the form of Ti at various stages of cycling. Effects of the environment and electron beam on the particles are also presented.

* Corresponding author. Tel.: +1 217 333 1440; fax: +1 217 333 2736.
E-mail address: ianr@uiuc.edu (I.M. Robertson).

0925-8388/$ – see front matter © 2007 Elsevier B.V. All rights reserved.
doi:10.1016/j.jallcom.2007.04.246

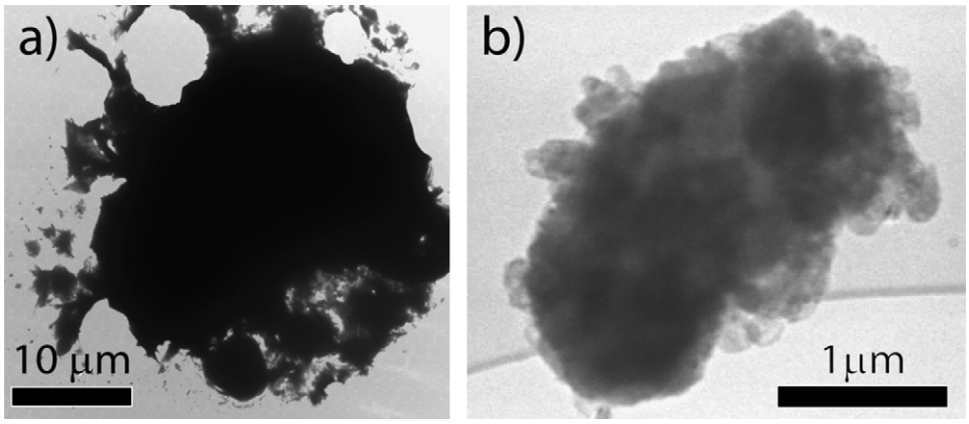

Fig. 1. (a) Bright-field TEM image of a $NaAlH_4$ particle after 1 h exposure to the environment and (b) bright-field TEM image of a particle transferred from the glove box to the TEM by using the transfer system.

2. Experimental

$NaAlH_4$ (Albemarle Corp.) and $TiCl_3$ (Aldrich Inc.) were mixed without further purification and placed in a 12 mL stainless steel bowl with seven 7-mm diameter stainless steel balls (ball-to-powder ratio varied between 30:1 and 40:1) to produce the samples. NaH (95%, ~200 mesh), Al powder (99.95%, ~200 mesh), and $TiCl_3$ were obtained from Aldrich Inc., mixed, and milled with the same parameters as above. After capping and sealing with Parafilm in the N_2-filled glove box, the bowls were loaded into a Fritsch 7 planetary mill and ball milled for 30 min at a rate of 350 rpm. Further details of this sample fabrication procedure are described in references [13,14].

The $NaAlH_4$ and the NaH + Al + 2 mol% $TiCl_3$ ("dehydrided" $NaAlH_4$) samples underwent cycles of hydrogenation and dehydrogenation with samples being stored after the 1st, 5th and 10th cycle. A volumetric pressure/composition/temperature (PCT) apparatus from Suzuki Shokan Co. measured pressure changes for H_2 wt.% calculations. Desorption began in vacuum at 160 °C and absorption started at 10 MPa H_2 gas at 120 °C. These samples were cycled to only 3 wt.% H_2 by overpressure due to a limitation in the dehydriding volume, which prevented dehydrogenation from proceeding to completion. The same conditions as above were also used with a PCT apparatus (LESCA Co.) which cycled the samples to their full 4 wt.% capacity to create six more samples after the 1st, 5th and 10th cycle.

For microanalysis, powder samples were pressed in to holey C grids inside an Ar-filled glove box. To minimize degradation due to environmental exposure, the grids were loaded in a Gatan heating and environmental cell TEM holder (HHST4004) in the Ar-filled glove box. The holder was then retracted into the cell and the cell evacuated to a roughing pump vacuum pressure. The transfer system was then transported to the electron microscope and the holder inserted into the column.

The microanalysis was conducted in a JEOL 2010F, which is a Schottkey field-emission gun transmission electron microscope. The instrument is equipped with an atmospheric thin window Si(Li) Oxford EDS detector and a Gatan Imaging Filter (90° magnetic sector), with ~0.3 eV/px dispersion at the charge coupled device. The latter detector was used for acquiring electron energy loss spectra. For EELS analysis, a core-loss spectrum was acquired starting at ~400 eV (including the Ti L-edge and O-K edge) and then a low-loss spectrum was recorded. Prior to each experiment with $NaAlH_4$, the electron energy loss spectrometer was aligned with TiO_2. The TiO_2 spectrum has characteristic "white lines" (5 eV peak-to-peak) that are a result of crystal-field splitting [29,30]. These lines were obtained to provide a test of resolution as well as ensuring the alignment of the microscope was optimized. The spectra were deconvolved by subtracting the reflected zero-loss tail from the low-loss spectrum. The post-edge structure of two different spectra can then be compared qualitatively [31]. The energy dispersive and electron energy loss spectra were acquired in scanning TEM mode. The probe current was ~0.5 nA and the probe diameter was 5 nm.

To enable identification of the form of the Ti, a series of standard spectra were acquired from Ti and Ti alloys as well as from precursor materials. Ti standards were cut from a block of commercially pure Ti, ground using standard metallographic techniques, and jet electropolished using a Tenupol 3 and a 10%/90% perchloric acid/methanol solution [32]. Spectra were also obtained from the hydrides introduced by jet electropolishing. Crushed Al_3Ti in both the metastable cubic and stable orthorhomic forms were provided by Dr. Hendrick Brinks [23]. TiO_2 (rutile) and $TiCl_3$ powders were purchased from Sigma–Aldrich. TiAl and Ti_3Al samples were obtained from prior experiments [33].

3. Results and discussion

The first concern was the stability of the particles to air exposure and to determine the best method of transporting the loaded TEM sample holder from the glove-box to the electron microscope. In Fig. 1, the microstructure of a $NaAlH_4$ particle that had been exposed to the atmosphere for 1 h (Fig. 1(a)) is compared to one that had been transferred directly to the microscope using the Gatan transfer system (Fig. 1(b)). The morphology and opacity of the two particles are different. The one exposed to the environment has clearly degraded whereas the one transferred using the Gatan stage has not. Short exposure times to the environment as well as the effectiveness of using an inert-gas filled glove bag to protect the sample during transport from the glove-box to the TEM were also assessed. It was found that the most effective method of transferring the sample was with the Gatan stage as there was always some uncertainty as to the cause of any difference detected in samples transferred using the other methods.

An additional complicating factor is the sensitivity of the particle to the electron beam; displacement damage, sputtering and local heating effects are all possible processes by which the particles could be degraded. For example, the bright-field images presented in Fig. 2 are frames captured from a digital video showing a crystal growing at 70 °C from a $NaAlH_4$ + 2 mol% $TiCl_3$ sample. EELS and EDS analysis identified this as a Na crystal. No crystals were visible upon the initial viewing of the sample. Slow growth of the crystals occurs over 20 min. The crystals were re-melted with approximately 2000 A/m^2 beam current density (a), and then large scale Na crystal growth occurs with a lower illumination intensity (b), with subsequent thickening and rotation towards the beam (accounting for the apparent

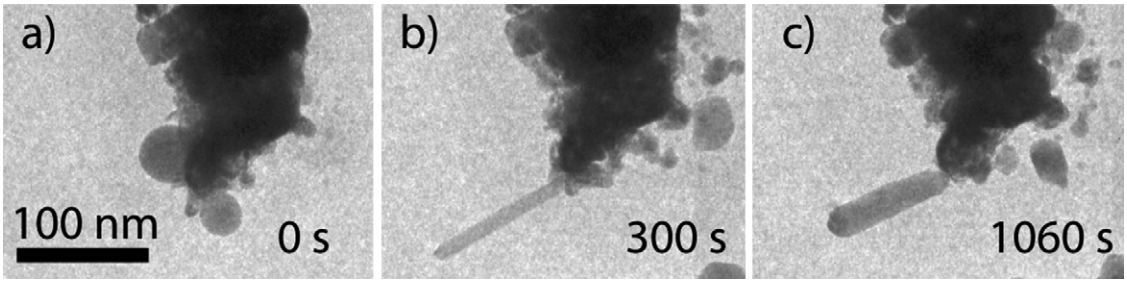

Fig. 2. (a–c) Na crystal growth from 10 cycle $NaAlH_4$ + 2 mol% $TiCl_3$, showing growth under the electron beam of a large crystal from the ball milled agglomerate. The sample temperature was 70 °C.

shortening in (c)). These effects also occur at room temperature, and are therefore due to beam displacements and not to the temperature. To minimize these effects, the area being analyzed must receive a minimum exposure to the electron beam. Unfortunately, this minimum exposure requirement impacts the signal-to-noise ratio which increases the minimum detectable mass fraction of an element. To enable detection of the elements, a compromise had to be made between beam exposure and data acquisition time.

Ti-rich regions in $NaAlH_4$ for EELS analysis were identified by first forming compositional maps of the $NaAlH_4$ by using EDS. Compositional EDS maps for particles of $NaAlH_4$ + 2 mol% $TiCl_3$ after 10 cycles of 3 wt.% H_2 and 4 wt.% H_2 are presented as Fig. 3(a) and (b), respectively. These maps appear to show a correlation between the locations of Ti and Cl; see, for example, the circled regions in Fig. 3(a). The possible correlation of the Ti is less apparent in the 4 wt.% H_2 sample. However, it must be remembered that the volume from which X-ray signals are generated extends through the thickness of the sample. Therefore, no definitive statement about the location or correlation of Ti and Cl can be made beyond they both exist within the same sampling volume.

Electron energy loss spectra of the standards are presented and compared in Fig. 4. The structure of the Ti peak approximately 10 eV after the onset of the L-edge changes distinctly for each standard, which permits them to be used as a fingerprint to identify the form of Ti as a function of the number of hydrogen cycles.

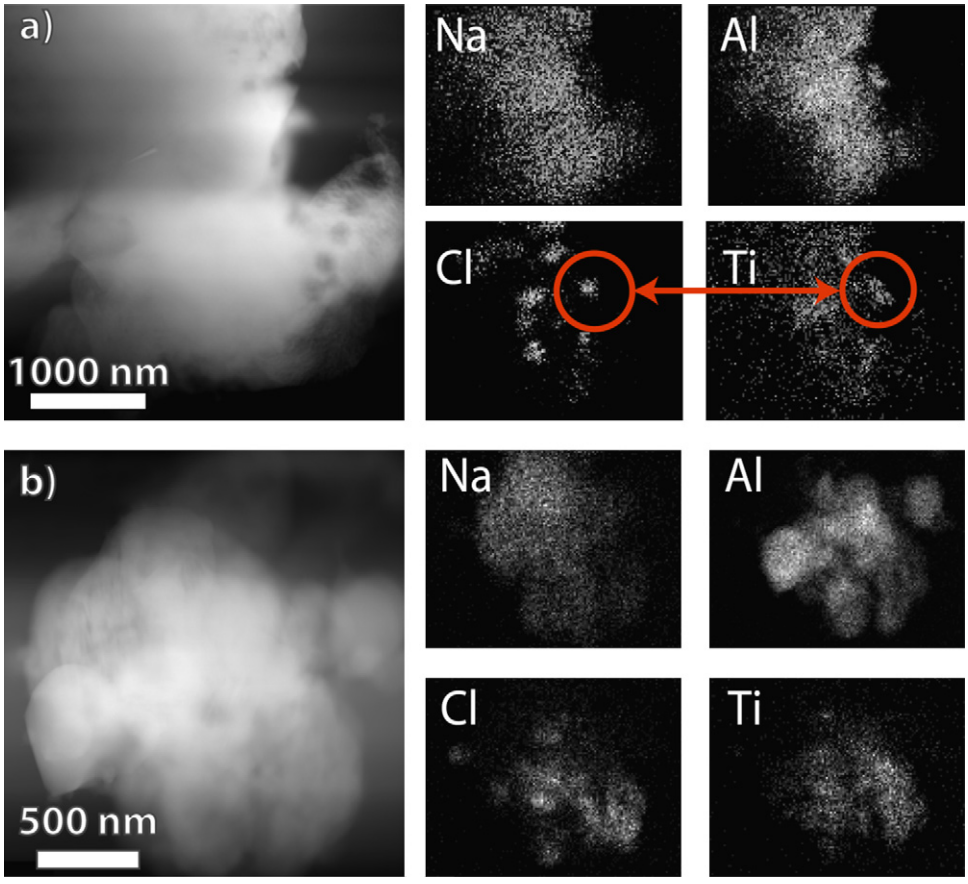

Fig. 3. EDS maps from (a) $NaAlH_4$ + 0.02 $TiCl_3$, 10 cycles, 3 wt.% H_2, and (b) NaH + Al + 0.02 $TiCl_3$, 10 cycles, 4 wt.% H_2, showing correlation in the chemical locations between Ti and Cl in both materials.

Table 1
Analyzed $NaAlH_4$ + 2 mol% $TiCl_3$ samples

Material	3 wt.%	4 wt.%	Cycles	Doping level
$NaAlH_4$	X		As-milled	2 mol% $TiCl_3$
$NaAlH_4$	X	X	1	2 mol% $TiCl_3$
$NaAlH_4$	X	X	5	2 mol% $TiCl_3$
$NaAlH_4$	X	X	10	2 mol% $TiCl_3$
NaH + Al ("dehydrided")	X		As-milled	2 mol% $TiCl_3$
NaH + Al	X	X	1	2 mol% $TiCl_3$
NaH + Al	X	X	5	2 mol% $TiCl_3$
NaH + Al	X	X	10	2 mol% $TiCl_3$

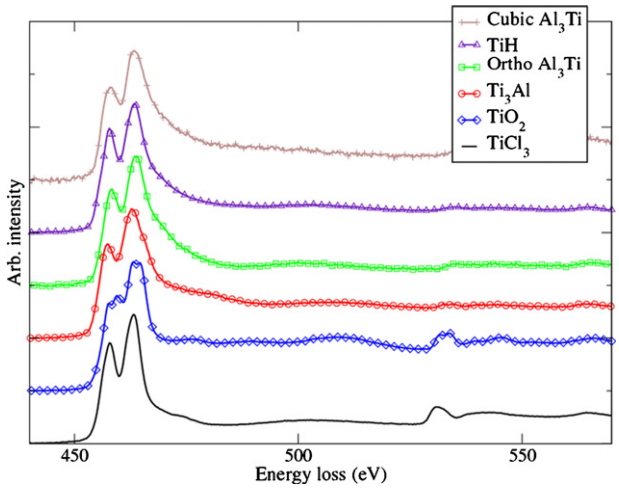

Fig. 4. EELS spectra of metallic and covalent standards used in this experiment. Note the distinct difference in post-edge structure.

Electron energy loss spectra were obtained from samples of $NaAlH_4$ + 2 mol% $TiCl_3$ after different numbers of hydrogen charging and discharging cycles; the conditions examined are summarized in Table 1. The regions from which electron energy loss spectra were acquired were those identified by EDS as containing Ti. Spectra from samples that had experienced different numbers of cycles are compared in Fig. 5. The post-edge structure for low-cycle (0, 1, and 5) $NaAlH_4$ and $TiCl_3$ at 3 wt.% H_2 is

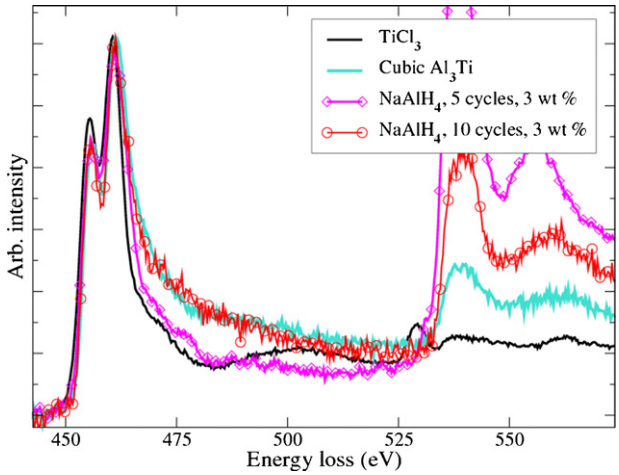

Fig. 5. Deconvolved spectra obtained from $NaAlH_4$ samples cycled at 3 wt.% overlaid on selected standards.

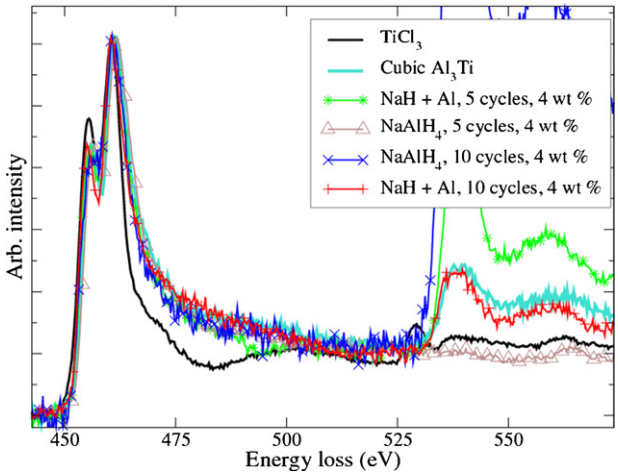

Fig. 6. Deconvolved spectra obtained from $NaAlH_4$ samples cycled at 4 wt.% overlaid on selected standards.

similar. With increasing number of cycles, there is a progressive change in the form of the Ti peak from $TiCl_3$-like to that of cubic Al_3Ti; the transition being complete between the 5th and 10th cycle. The transition to Al_3Ti is faster in materials that during cycling released 4 wt.% H_2, as shown by a comparison of the spectra in Fig. 6 to those in Fig. 5. Occasionally, some regions of TiO_2 were identified along the edges of particles. These are most likely attributable to the susceptibility of $TiCl_3$ to oxidation and indicate that even with the precautions taken in this study, some oxidation occurs. A null but important result was that no Ti was detected by using EELS in regions between those identified by EDS as being Ti rich. This result places a limit on the minimum amount of Ti that must be present in these regions. The Ti concentration within these regions is currently being determined by assessing the concentration of Ti partitioned to Al_3Ti and TiO_2 and subtracting it from the amount introduced as well as by calculating the minimum detectable mass fraction by EDS and EELS. This will allow limits on the amount of "free" Ti to be estimated.

4. Conclusion

Microchemical information from environment-sensitive complex metal hydride storage materials is possible within the electron microscope by using a transfer system to minimize exposure to air between the glove-box and the electron microscope. Thus, evidence from TEM analysis of an oxide, especially

one that covers the particle should be interpreted cautiously as this may occur prior to insertion of the sample in to the instrument. The dominant form of Ti is Al_3Ti within $NaAlH_4$, although the presence of some TiO_2 is detected along the sample edges. The existence of Al_3Ti and the increase in volume fraction with increasing number of hydrogen charging/discharging cycles suggests that it is not the catalytic form of Ti as Al_3Ti likely has a low activity for H_2 and the surface is most probably alumina, which is an effective barrier to hydrogen. The presence of TiO_2 will not inhibit hydrogen uptake to any significant extent but it is unlikely to be the catalytic form of Ti [33]. The existence of a solid solution of $Al_{1-x}Ti_x$ cannot be ruled out from this preliminary data despite the observation that no evidence was found for Ti existing in regions other than those identified by EDS as containing Ti. Work is currently in progress to estimate the level of unbound Ti and to assess if it is sufficient to be detected by EELS or EDS.

Comparison of the samples cycled at 3 and 4 wt.% H_2 suggest that the formation of Al_3Ti is much faster with full cycles. One possible explanation of this effect is that less Al segregation occurs when dehydrogenation is limited to 3 wt.%, so less metallic Al is available to react with $TiCl_3$. It is also possible that, with only reaction (1) occurring in a 3 wt.% H_2 sample, the formation of Al_3Ti preferentially occurs during reaction (2):

$$NaAlH_4 \leftrightarrow 1/3Na_3AlH_6 + 2/3Al + H_2 \quad (3.7\,\text{wt.\%}\,H_2) \quad (1)$$

$$Na_3AlH_6 \leftrightarrow 3NaH + Al + 3/2H_2 \quad (1.9\,\text{wt.\%}\,H_2) \quad (2)$$

In situ discharge experiments are in progress to determine if the redistribution of the elements that accompanies hydrogen discharging can be detected.

Acknowledgements

This research was carried out with the support of the US Department of Energy for DDG and IMR under grant DE-FC36-056015064. LFC, MS, and CMJ gratefully acknowledge the support of the Office of Hydrogen, Fuel Cells, and Infrastructure technologies of the US DOE. A majority of the research in this paper was carried out in the Center for Microanalysis of Materials, University of Illinois, which is partially supported by the U.S. Department of Energy (DOE) under grant DEFG02-91-ER45439.

References

[1] B. Bogdanovic, M. Schwickardi, J. Alloys Compd. 253–254 (1997) 1–9.
[2] C.M. Jensen, R. Zidan, N. Mariels, A. Hee, C. Hagen, Int. J. Hydrogen Energy 24 (1999) 461–465.
[3] R.A. Zidan, S. Takara, A.G. Hee, C.M. Jensen, J. Alloys Compd. 285 (1999) 119–122.
[4] B. Bogdanovic, R.A. Brand, A. Marjanovic, M. Schwickardi, J. Toelle, J. Alloys Compd. 302 (2000) 36–58.
[5] C.M. Jensen, K.J. Gross, Appl. Phys. A 72 (2001) 213–219.
[6] B. Bogdanovic, M. Schwickardi, Appl. Phys. A (Mater. Sci. Process.) A72 (2001) 3.
[7] G. Sandrock, K. Gross, G. Thomas, C. Jensen, D. Meeker, S. Takara, Proceedings of the International Symposium on Metal-Hydrogen (MH 2000), Elsevier Science Ltd., Noosa Heads, AU, 2002.
[8] K.J. Gross, G.J. Thomas, C.M. Jensen, J. Alloys Compd. 330–332 (2002) 683–690.
[9] G. Sandrock, K. Gross, G. Thomas, J. Alloys Compd. 339 (2002) 299–308.
[10] M. Fichtner, O. Fuhr, O. Kircher, J. Rothe, Nanotechnology 14 (2003) 778–785.
[11] S.S. Srinivasan, H.W. Brinks, B.C. Hauback, D. Sun, C.M. Jensen, J. Alloys Compd. 377 (2004) 283–289.
[12] P. Wang, C.M. Jensen, J. Alloys Compd. 379 (2004) 102.
[13] P. Wang, C.M. Jensen, J. Phys. Chem. B 108 (2004) 15827–15829.
[14] M.T. Kuba, S.S. Eaton, C. Morales, C.M. Jensen, J. Mater. Res. 20 (2005) 9.
[15] S. Gomes, G. Renaudin, H. Hagemann, K. Yvon, M.P. Sulic, C.M. Jensen, J. Alloys Compd. 390 (2005) 305–313.
[16] O. Palumbo, R. Cantelli, A. Paolone, C.M. Jensen, S.S. Srinivasan, J. Phys. Chem. B 109 (2005) 1168–1173.
[17] C. Jensen, R. Zidan, 2002, 6471935, USA.
[18] H.W. Brinks, B.C. Hauback, C.M. Jensen, R. Zidan, J. Alloys Compd. 392 (2005) 27–30.
[19] S.V. Alapati, J.K. Johnson, D.S. Sholl, J. Phys. Chem. B 110 (2006) 8776.
[20] S. Chaudhuri, J.T. Muckerman, J. Phys. Chem. B 109 (2005) 6952–6957.
[21] W.G. Moffat, The Handbook of Binary Phase Diagrams, Genium Publishing Corporation, 1976.
[22] A. Leon, O. Kircher, J. Rothe, M. Fichtner, J. Phys. Chem. B 108 (2004) 16372–16376.
[23] J. Graetz, A.Y. Ignatov, T.A. Tyson, J.J. Reilly, J. Johnson, Materials for Hydrogen Storage, Materials Research Society, Boston, MA, 2004.
[24] J. Graetz, J.J. Reilly, J. Johnson, A.Y. Ignatov, T.A. Tyson, Appl. Phys. Lett. 85 (2004) 500–502.
[25] H.W. Brinks, C.M. Jensen, S.S. Srinivasan, B.C. Hauback, D. Blanchard, K. Murphy, J. Alloys Compd. 376 (2004) 215–221.
[26] G.J. Thomas, K.J. Gross, N.Y.C. Yang, C. Jensen, Proceedings of the International Symposium on Metal-Hydrogen (MH 2000), Elsevier Science Ltd., Noosa Heads, AU, 2002.
[27] C.M. Andrei, J.C. Walmsley, H.W. Brinks, R. Holmestad, D. Blanchard, B.C. Hauback, G.A. Botton, J. Phys. Chem. B 109 (2005) 4356.
[28] C.M. Andrei, J.C. Walmsley, H.W. Brinks, R. Holmestad, S.S. Srinivasan, C.M. Jensen, B.C. Hauback, Appl. Phys. A: Mater. Sci. Process. 80 (2005) 709–715.
[29] R.D. Leapman, L.A. Grunes, P.L. Fejes, Phys. Rev. B (Conden. Matter) 26 (1982) 614–635.
[30] C.C. Ahn, O.L. Krivanek, R.P. Burgner, M.M. Disko, P.R. Swann, EELS Atlas, Gatan Inc., 1983.
[31] R.F. Edgerton, Electron Energy-Loss Spectroscopy in the Electron Microscope, Plenum Press, New York, 1986.
[32] J.W. Edington, K.C. Thompson-Russel, Electron Microscope Specimen Preparation Techniques in Materials Science, Macmillian, 1975.
[33] D. Legzdina, I.M. Robertson, H.K. Birnbaum, Acta Mater. 53 (2005) 601–608.